New Hampshire DOT

Research

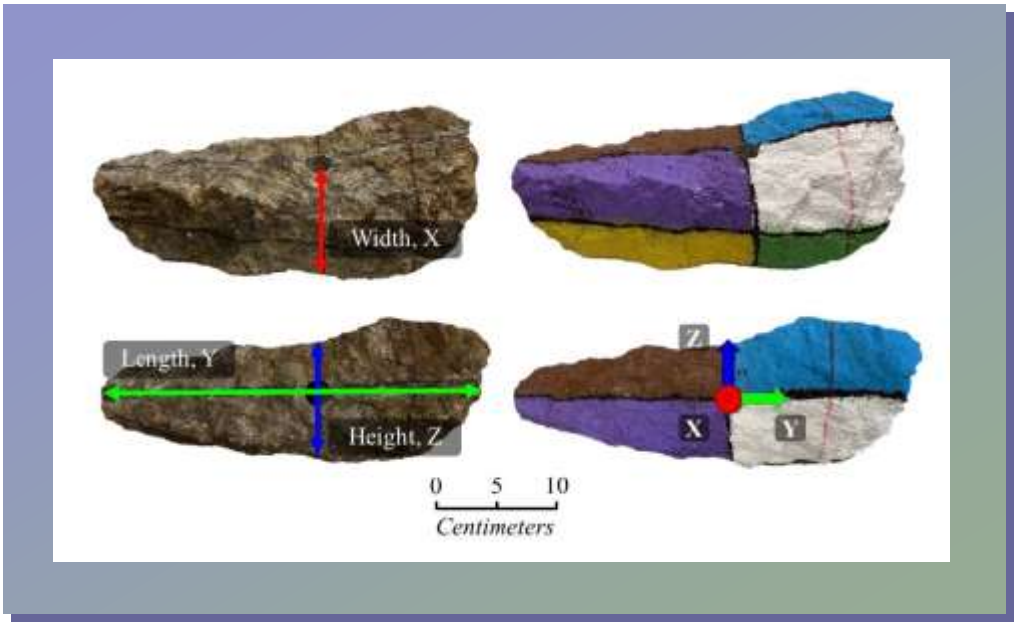

Use of Smart Rocks to Improve Rock Slope Design

Final Report

Prepared by University of New Hampshire Department of Civil and Environmental Engineering, College of Engineering and Physical Sciences, in cooperation with the U.S. Department of Transportation, Federal Highway Administration

Technical Report Documentation Page

1. Report No.	2. Gov. Accession No.	3. Recipient's Catalog No.
FHWA-NH-RD-26962Z		

4. Title and Subtitle	5. Report Date
Use of Smart Rocks to Improve Rock Slope Design	March 2022
	6. Performing Organization Code

7. Author(s)	8. Performing Organization Report No.
Jean Benoit and Bruma Souza	

9. Performing Organization Name and Address	10. Work Unit No. (TRAIS)
University of New Hampshire Department of Civil and Environmental Engineering Kingsbury Hall, 33 Academic Way Durham, New Hampshire 03824	11. Contract or Grant No. 26962Y, A004(857)

12. Sponsoring Agency Name and Address	13. Type of Report and Period Covered
New Hampshire Department of Transportation Bureau of Materials & Research Box 483, 5 Hazen Drive Concord, New Hampshire 03302-0483	FINAL REPORT 14. Sponsoring Agency Code

15. Supplementary Notes

Conducted in cooperation with the U.S. DEPARTMENT OF TRANSPORTATION, FEDERAL HIGHWAY ADMINISTRATION

16. Abstract

Rock slopes pose a hazard to the traveling public when weathering processes dislodge portions of the slope that can fall into the road. Both the design of new rock slopes and the hazard assessment of existing rock slopes need improvement to increase safety against rockfall, construct better engineered slopes and reduce short- and long-term maintenance costs.

This research summarizes rockfall assessments performed with the aid of Smart Rock sensors. The Smart Rock is a sensor system equipped with a 3-axis accelerometer and gyroscope, embedded in a regular rock, to measure impact (acceleration) and rotational velocity (gyroscope). These devices were used to evaluate rockfall events from the perspective of the falling rock.

More than 85 field experiments conducted in NH and VT provided Smart Rock data on rockfall, coupled with field measurements and video analysis. Some laboratory and modeling assessments were also undertaken to compare experimental trajectories with rockfall simulations.

The findings of this study confirm that, although rockfall events can be unpredictable, acceleration and rotational velocity data from the rock perspective present a high potential to expand rockfall understanding and improve model simulations. Acceleration and rotational velocity measurements from a Smart Rock were used to distinguish rockfall movement over time (free fall, bouncing, rolling, sliding). Predominant rockfall modes of motion were identified at different ranges of slope angles. These ranges were compatible with field and model observations published in the literature since the 1960s.

17. Key Words	18. Distribution Statement
Landslides, Rockfalls, Rockslides	No Restrictions. This document is available to the public through the National Technical Information Service (NTIS), Springfield, Virginia, 22161.

19. Security Classif. (of this report)	20. Security Classif. (of this page)	21. No. of Pages	22. Price
UNCLASSIFIED	UNCLASSIFIED	52	

Use of Smart Rocks to Improve Rock Slope Design

Jean Benoit

Bruma Souza, MSc

University of New Hampshire
Department of Civil and Environmental Engineering
Kingsbury Hall, 33 Academic Way
Durham, New Hampshire 03824

DISCLAIMER

USE OF SMART ROCKS TO IMPROVE ROCK SLOPE DESIGN

By

Project Investigator: Jean Benoît, Professor Emeritus

and

Graduate Student: Bruma Souza, MSc

University of New Hampshire

FINAL REPORT

Submitted to the New Hampshire Department of Transportation

Bureau of Materials and Research

Project # SPR 26962Z

March 2022

EXECUTIVE SUMMARY

This Research Report was submitted to the New Hampshire Department of Transportation to summarize rockfall assessments performed by the University of New Hampshire with the aid of Smart Rock (SR) sensors. These sensors consist of 3D printed capsules 50.8 mm in length and 25.4 mm in diameter, equipped with a ±400 g and a ±16 g 3-axis accelerometer, a ±4000 dps high-rate gyroscope, and an altimeter. These devices were used to evaluate rockfall events from the perspective of the falling rock.

More than 85 field experiments conducted in NH and VT provided SR data on rockfall at 10 different sites with a wide range of topographies and geological conditions, coupled with field measurements and video analysis. Some laboratory and modeling assessments were also undertaken to compare experimental trajectories with rockfall simulations.

The findings of this study confirm that, although rockfall events can be unpredictable, acceleration and rotational velocity data from the rock perspective present a high potential to expand rockfall understanding and improve model simulations. Acceleration and rotational velocity measurements from a Smart Rock were used to distinguish rockfall movement over time (free fall, bouncing, rolling, sliding). Predominant rockfall modes of motion were identified at different ranges of slope angles. These ranges were compatible with field and model observations published in the literature since the 1960s.

The modes of motion of a rockfall and the site characteristics exert a significant effect on the distances traveled by falling blocks. Shallower slopes and the presence of slope irregularities often increased runout distances and horizontal displacements. It was also demonstrated that rockfall motion is strongly influenced by the characteristics of the falling block and its fall kinematics. Lighter blocks typically experienced higher rotation and impact accelerations.

ACKNOWLEDGEMENTS

The support for this research project by the New Hampshire Department of Transportation Bureau of Materials and Research is greatly appreciated. Special thanks to the members of the Smart Rock Technical Advisory Group for their time, interest, support, and collaboration: Krystle Pelham, Neil Olson, Deirdre Nash, Ann Scholz, David Scarpato, Kevin Coyle, Jay Levine, Dan Prehemo, and Dennis Herrick. We would also like to acknowledge Artur Apostolov, Noah MacAdam, Hannah Miller, the Vermont Agency of Transportation, and Ameritech for their technical support and assistance during testing.

TABLE OF CONTENTS

LIST OF TABLES

LIST OF FIGURES

1. INTRODUCTION

Rockfalls are becoming increasingly of concern as climatic changes lead to further erosion of slopes, cliffs, and rocky terrains (Caviezel et al., 2018). The risk of damage increases near roads or in areas with significant population density (Azzoni et al., 1995), thus increasing infrastructure demand (Heidenreich, 2004; Garcia, 2019). Falling blocks present considerable economic impact (Turner and Jayaprakash, 2012), and these regions demand thorough knowledge concerning rockfall trajectories, hazard mapping, and effective rockfall defense systems (Heidenreich, 2004).

Rockfall events were not systematically investigated until the 1960s. Ritchie (1963) evaluated falling blocks and developed a research program that became one of the most significant rockfall engineering milestone. Ritchie identified that falling blocks could experience one or more modes of travel, including free-fall, bouncing, rolling, and sliding. Potential rockfall locations typically reflect the behavior identified by Ritchie (1963): upper, steeper slopes as a source location for initial free fall, followed by a transition zone with moderate inclinations where the rocks can bounce, and a final runout zone where the blocks can roll and slide as they decelerate before ultimately coming to rest.

The first stage during a rockfall occurrence is the detachment of the block from the slope, which generally occurs along discontinuities (e.g., joints, fractures, bedding planes). Next, rock movement happens following an initial rolling or sliding stage, usually attributed to a variation in slope angle or motion from a previous impact. Next, falling blocks experience translational (linear displacement of the center of mass) and rotational (angular displacement around the center of mass) movements, which in the field occurs three-dimensionally.

Proper protection design requires information about rockfall energy and trajectory (Wyllie, 2015). However, the trajectories followed by falling blocks are complex and still not well-

understood (Chau et al., 2003; Heidenreich, 2004; Labiouse and Heidenreich, 2009; Higgins and Andrew, 2012; Disenhof, 2018; Garcia, 2019). The present-day mitigation and protective designs are based on kinetic energy estimates, which typically disregard or inaccurately predict inherent and essential aspects of rockfall modeling such as rotational energy and rock rebound (Chau et al., 2003; Turner and Duffy, 2012).

In addition to overly conservative simulation models, current rockfall analysis methods typically include field and/or laboratory measurements, high-frame video recording systems, and detailed event back-analyses. However, these techniques rarely provide detailed information about rock-surface interaction and translational and rotational rock kinematics (Caviezel and Gerber, 2018). To address this issue, researchers have started to instrument rocks with Inertial Measurement Units (IMUs), including triaxial accelerometers and gyroscopes for precise information regarding rock rotation and impact (Apostolov, 2016; Caviezel et al., 2017; Caviezel and Gerber, 2018; Caviezel et al., 2018; Disenhof, 2018).

Research conducted at the University of New Hampshire (Durham, NH) since the early 2000s has developed and improved several generations of Smart Rock (SR) sensors. SRs can instrument test rocks in field and laboratory rockfall experiments from the falling rock perspective (Harding, 2011; Cassidy, 2013; Gullison, 2013; Harding et al., 2014; Apostolov, 2016; Apostolov and Benoît, 2017; Disenhof, 2018). The early generation smart rocks were designed for use in landslide studies (Gullison, 2013; Harding et al., 2014; Coombs et al., 2020) until research efforts shifted to rockfall with further refinements in the sensor capabilities. The latest SRs are equipped with accelerometers, a gyroscope, and an altitude sensor.

In the research described in this report, several instrumented rockfall experiments were carried out on ten rock slopes in New Hampshire and one in Vermont. The field tests were

conducted with Smart Rock sensors embedded in the center of gravity of local rocks retrieved at each slope location. Preliminary laboratory assessments were performed after the field trials to establish a research methodology capable of evaluating instrumented rock rebounds accurately and consistently. Finally, the experimental trajectories and rotation motion were compared with rockfall simulations using default input parameters and energy restitution coefficients estimated in the laboratory.

1.1. Objectives

Preliminary work performed at the University of New Hampshire in collaboration with the NHDOT has shown that using a Smart Rock sensor embedded in natural rocks can provide the necessary field response data to calibrate and revise existing rockfall simulation software models (Disenhof, 2018). To achieve this primary goal of improving rock slope design, this project had the following objectives:

- Improve the current Smart Rock sensors to include altimeter capacity.
- Conduct multiple experiments with the Smart Rock at 10 rock cuts rated A or B according to the New Hampshire RHRS.
- Analyze the Smart Rock accelerometer and gyroscope data coupled with video recording of each experiment to extract information and parameters as input to current rockfall software packages.
- Develop a design evaluation protocol for new and existing slopes using Smart Rock technology.

This report describes how each of these objectives were met through experiments and analyses conducted by researchers at the University of New Hampshire.

2. FIELD METHODOLOGY

A series of 85 field rockfall experiments were carried out on ten rock cuts in New Hampshire and one in Vermont using the fourth-generation SRs. The test slopes encompassed a wide variety of characteristics, including slope height, slope inclination, irregularities in geometry, geology, protective ditch, and presence of road nearby. These field trials were conducted to evaluate how rock motion occurs under different site conditions. Each test was video recorded and performed with the aid of a Smart Rock sensor embedded in field-collected rocks from each site. Details regarding the Smart Rock sensor, rock preparation and test procedures are discussed in the following sections.

2.1. Smart Rock sensor

Smart Rock (SR) sensors are small, fully autonomous devices, applicable to a wide variety of geotechnical problems where motion tracking is needed, such as landslides, debris flow, and rockfalls (Apostolov, 2016; Apostolov and Benoît, 2017). There are currently five generations of Smart Rock sensors. The first two generations of SRs were initially designed to track the position of soil particles over time during debris-flow flume experiments (Harding, 2011; Cassidy, 2013; Gullison, 2013; Harding et al., 2014).

Further sensor improvements led to the third-generation SR, applicable to both debris flow and rockfall experiments (Apostolov, 2016; Disenhof, 2018; Coombs et al., 2020). The fourth-generation SRs were embedded in test rocks and used to investigate rockfall events. They consist of 3D printed capsules 50.8 mm in length and 25.4 mm in diameter (Figure 1). Each SR is equipped with a ±400 g and a ±16 g 3-axis accelerometers, a ±4000 degrees per second (dps) high-rate gyroscope, and an altimeter. Recently, a fifth-generation Smart Rock sensor (Figure 1b) was

developed with doubled battery autonomy, and physical modifications to include a retrieval hook and printed axes orientations on the capsules.

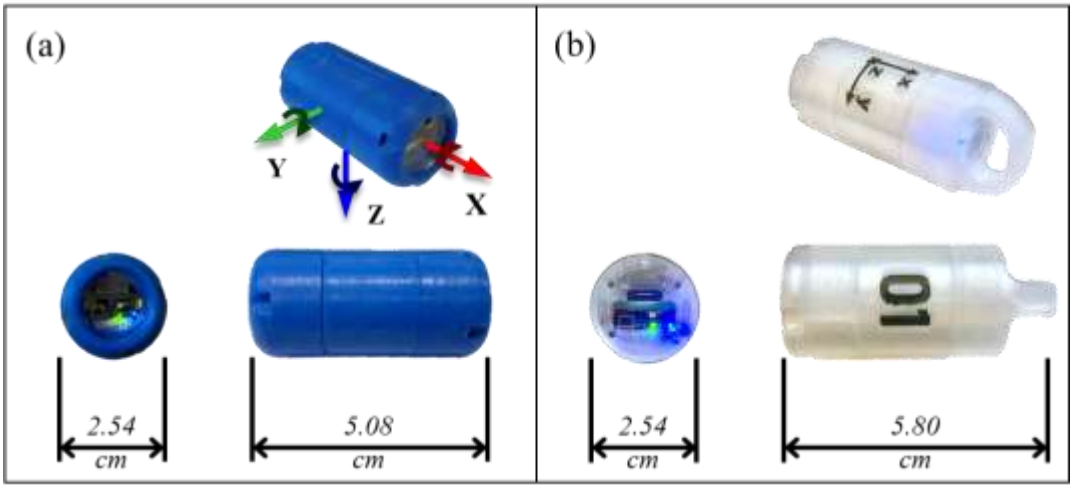

Figure 1. (a) Fourth- and (b) fifth-generation Smart Rock sensors.

The dual accelerometers allow the SR to capture the full range of accelerations rocks may experience during a rockfall. While the ±400 g accelerometer captures more significant magnitude accelerations produced by higher impacts from a fall or a bounce, the ±16 g accelerometer captures smaller magnitude accelerations not gathered from the high-g accelerometer. The low-g accelerometer presents a significant advantage in evaluating the rock behavior as it allows users to identify whether the rock is in free fall (0 g) or at rest (1 g). In order to decrease noise in the low-g acceleration signal, the recording was purposely limited to ±8 g.

The high-rate gyroscope provides instantaneous rotation rates about the three axes in degrees per second, simultaneously. The altimeter allows for tracking changes in altitude and requires the sensor to be open to the atmosphere using a hole in the SR plexiglass window.

The latest SRs are simple to operate and process data in real-time. A Smart Rock records data at a sampling frequency of 100 Hz (used in this research), which can be increased to 500 Hz if the altimeter is not used. The recorded motion is automatically saved to a micro-SD card as a

.csv file to be analyzed using MATLAB. For additional information about the latest generations of SRs, the reader is referred to Apostolov (2016) and Apostolov and Benoît (2017).

2.2. Experimental methodology

2.2.1. Site selection

There are approximately 375 rock cuts along transportation corridors in New Hampshire, tracked and rated using the Rockfall Hazard Rating System (RHRS) in a database maintained by the Bureau of Materials and Research of the NHDOT. The RHRS classifies the rockfall hazard levels as A (high), B (moderate), or C (low). For rock cuts taller than 8 meters, 11% of the monitored rock slopes in NH were rated A, 27% were rated B, while the remaining 62% were rated C. In this rockfall assessment, priority was given to medium-to-high hazard slopes provided by the NHDOT, whose characteristics are shown in Table 1.

2.2.2. Preparation of test rocks

The test rocks used in the field experiments were retrieved from each slope location to match the slope composition. In addition, a 5 kg metamorphic test rock referred to as “reference rock” was used in these experiments for site-to-site comparison purposes. Each test rock was drilled in its center of gravity (CG) to avoid eccentricity from SR measurements during the tests. The CG position of each test rock was determined from hand-drawn cross-sections and 3D models of each test block.

The test rocks were drilled with a 25.4 mm outer diameter core bit, using an adjustable rock borer frame to control the drilling location and angle. In addition, density measurements were performed using the recovered rock cores. For more efficient video analysis, the center of gravity

location was marked on each rock about three different directions, and the eight resultant quadrants were painted in different colors (Figure 2). As shown in the figure, the width, length, and height of the test block at the CG lines (visible in black) were measured in the X, Y, and Z orientations of the Smart Rock embedded in each block, respectively. Finally, the shape of each rock was determined based on the particle shape classification diagram developed by Sneed and Folk (1958), shown in Figure 3.

Table 1. Test site information.

Slope ID, rating	**Rock type**	**Slope height (m)**	**Slope angle**	**Catchment ditch**		**Road present?**	**Protective structure?**	**Number of tests**
				Type	**Width (m)**			
Dover, NH Not rated	Metamorphic	9.0	50º to 60º	Rock talus	-	No	No	4
Danbury, NH A-rated	Igneous	10.5	70º to 75º	Grass	2.0	Yes	No	9
Franconia, NH B-rated	Igneous / Metamorphic	9.5	25º to 90º	Grass / Soil	10.0 / 1.5	Yes	No	12
Franklin 1, NH A-rated	Metamorphic	12.5	45º to 90º	Soil with grass	1.3	Yes	No	8
Franklin 2, NH A-rated	Metamorphic	10.0	50º to 60º	Soil with vegetation	2.5	Yes	No	7
Franklin 3, NH A-rated	Metamorphic	18.0	40º	Soil with vegetation	3.0	Yes	No	7
Keene, NH C-rated	Igneous	10.0	70º to 75º	Soil	-	No	No	8
Orange, NH B-rated	Igneous / Metamorphic	9.0	65º to 75º	Soil with vegetation	5.0	Yes	No	7
Warner, NH A-rated	Igneous	15.0	70º to 85º	Soil	3.5 to 5.0	Yes	No	8
Windham, NH B-rated	Metamorphic	12.5	60º to 65º	Rock talus	2.0	No	No	7
Townshend, VT A-rated	Metamorphic	19.0	30º to 80º	Boulders	2.5	Yes	Yes	8
							Total number of tests	85

In this research, 56 local rocks were prepared in the laboratory prior to the field experiments. The test blocks were selected for each site based on their size. They needed to be large enough to house the SRs and small enough to be manually hoisted or hand-carried to the top of the slopes. The igneous and metamorphic nature of the test rocks was dependent on the geology of rock slopes near roads typically encountered in New Hampshire.

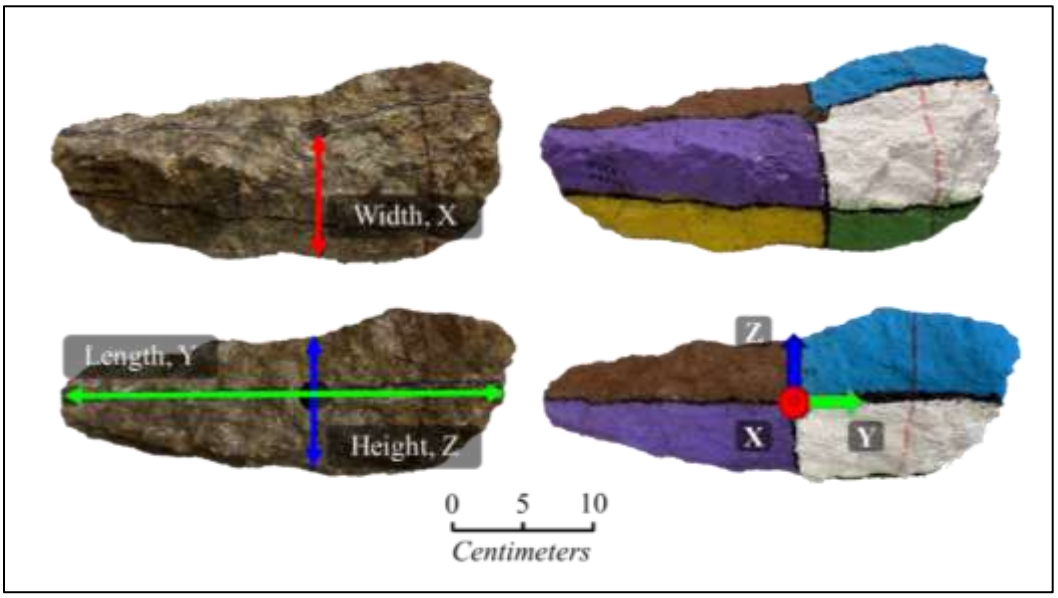

Figure 2. Test rock prepare for field experiments in Warner, NH. The X, Y, Z coordinate system indicates the SR orientation. Each test rock was painted in eight different colors (two quadrants are not visible in the figure) to identify the sensor orientation in video.

The maximum and minimum dimensions of the tested rocks varied between 10 and 45 cm, with an average side of 20 ± 10 cm, while the masses of the blocks ranged between 4 and 30 kg and averaged 11 ± 6 kg. Two experimental rockfalls were also performed with larger blocks in-place during scaling work (Figure 4). Due to the impossibility of accurately determining the CG location of larger blocks, the approximate CG drilling position for these blocks was determined visually.

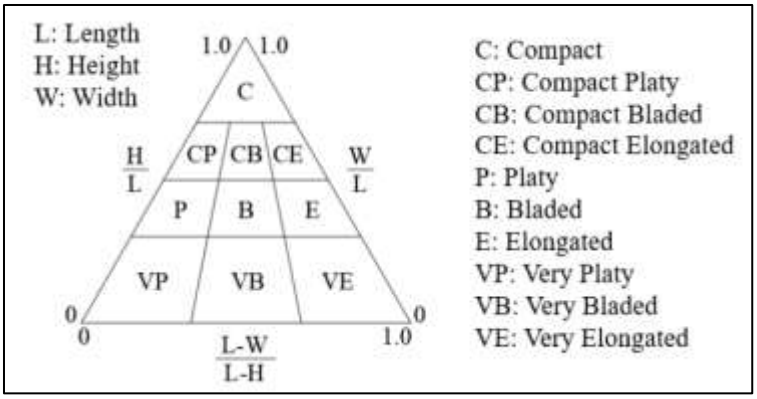

Figure 3. Particle shape classification diagram adapted from Sneed and Folk (1958).

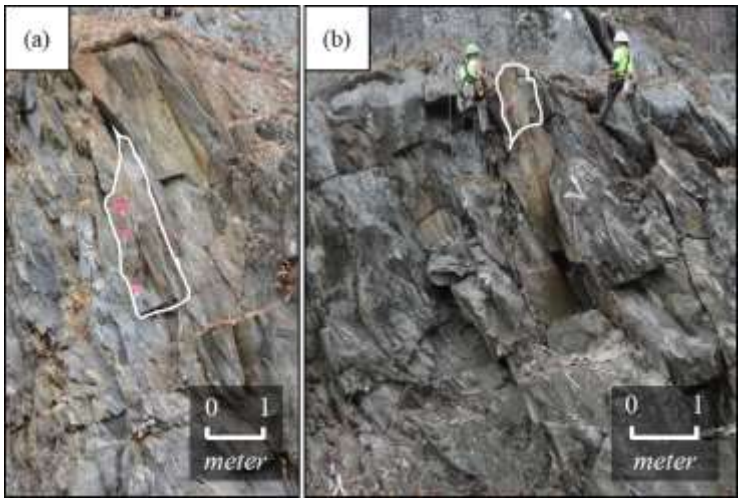

Figure 4. Scaled blocks in Townshend, VT. The pink dots indicate the SR locations.

2.2.3. Field tests

Before starting each test, the Smart Rock was activated and self-calibrated. The SR was placed inside the drilled holes, and a 25.4 mm diameter expandable rubber plug with a through-hole screw was used to confine the SR. After each rock was prepared, a pulley, rope, and bucket were used to hoist them to the top of the slope, and larger rocks were hand-carried.

To help identifying the beginning of each experiment, the test operator tapped the rock onto the slope surface three times to indicate the start of each test in the data signal; then, the block was released from the slope with the least initial velocity possible. During release, each test block

was positioned so that the Smart Rock sensor hole was facing the road, and the longest axis of the test rock was parallel to the rock slope face. After rockfall, the runout distance as well as lateral dispersion from the slope toe were measured, and the SR was extracted from the rock. Although a small number of test rocks suffered fragmentation, this phenomenon was not analyzed in this preliminary research.

All field experiments were video recorded at 30 fps (frames per second) perpendicularly to the slope face. Rock movement could be tracked using the application Tracker 5.1.5 by Physlets. It assumes the camera is stationary and perpendicular to the object in motion and provides vertical and horizontal displacement and velocity data over time by tracking the rock CG position at each frame.

2.2.4. Data processing

The Smart Rock data is saved as a .csv file and stored to a microSD card, which can be removed after each test is recorded. The raw data for each rockfall test were processed and plotted using MATLAB. After selecting the time intervals of interest for data analysis, the script calculates relevant aspects from the sensor data, such as resultant acceleration and rotation. The resultant acceleration vector is composed of both low- and high-g accelerometers, in which low-g acceleration resultants higher than 8 g were replaced by the high-g resultant acceleration.

The resultant acceleration data also provides information to estimate impact forces to a surface or barrier, which are relevant for protective design against rockfall. These respective resulting g-forces can be converted to force intensities using the rock mass and gravity acceleration ($g = 9.81$ m/s², SI units) in Equation 1. Estimating impact forces is fundamental in the design of protective structures, especially at less inclined slopes where higher horizontal motion is likely to

be developed. For more details on the retrieved sensor and video test data analysis, the reader is referred to Chapter 4 of Souza (2021).

$$Impact\ force = \left(Resultant\ g_{force}\right) * 9.81 * (rock\ mass) \quad \text{(Equation 1)}$$

3. EXPERIMENTAL ROCKFALLS

3.1. Smart Rock data

This section describes one of the test sites where eight field rockfall tests were conducted on a 15 m tall, A-rated granodiorite rock cut in Warner, NH. The rock face is located parallel to NH Route 103 and has a 3.5 to 5 m wide flat catchment ditch constructed with granular soil. The slope has an average inclination between 70º and 85º. Traffic control was required during the rockfall experiments due to the proximity of the slope to the road. An example of video and sensor data compatibility is shown in Figures 5 and 6 for an 18 kg bladed rock.

The tracking software output was used to evaluate rockfall motion in conjunction with the data from the SR sensors. Figure 5 establishes a comparison between the observed trajectory combining selected video frames (Figure 5a) and using the tracker software (Figure 5b), while Figure 6 presents the sensor output after data processing, as well as the corresponding modes of motion at each time frame. The letters A through D in both figures indicate the different rockfall stages, matched through both SR and video recording times.

Rock 6 has experienced a wide range of rockfall motion, which could be identified in both video and sensor signals. The flat acceleration (1 g) and rotational velocity (0 dps) lines indicate that the rock is at rest. After being released from the top of the rock cut at 0.8 s, the rock initially rolled down a roughly 60º inclined surface (A). It is possible to observe an increase in the revolution rate with the downward movement and small acceleration peaks that do not exceed ±8 g, likely due to surface roughness and irregular test rock shape. The rock then bounced four times on the rock face (B), with visible changes in rotation after each impact, and fell freely for 2 s (C) at 0 g. The test rock then hit the ground surface at 3.7 s (D). After the impact on the ground 1.3 m from the slope toe, the rock was embedded 10 cm in the soil, and no kinetic energy was restituted.

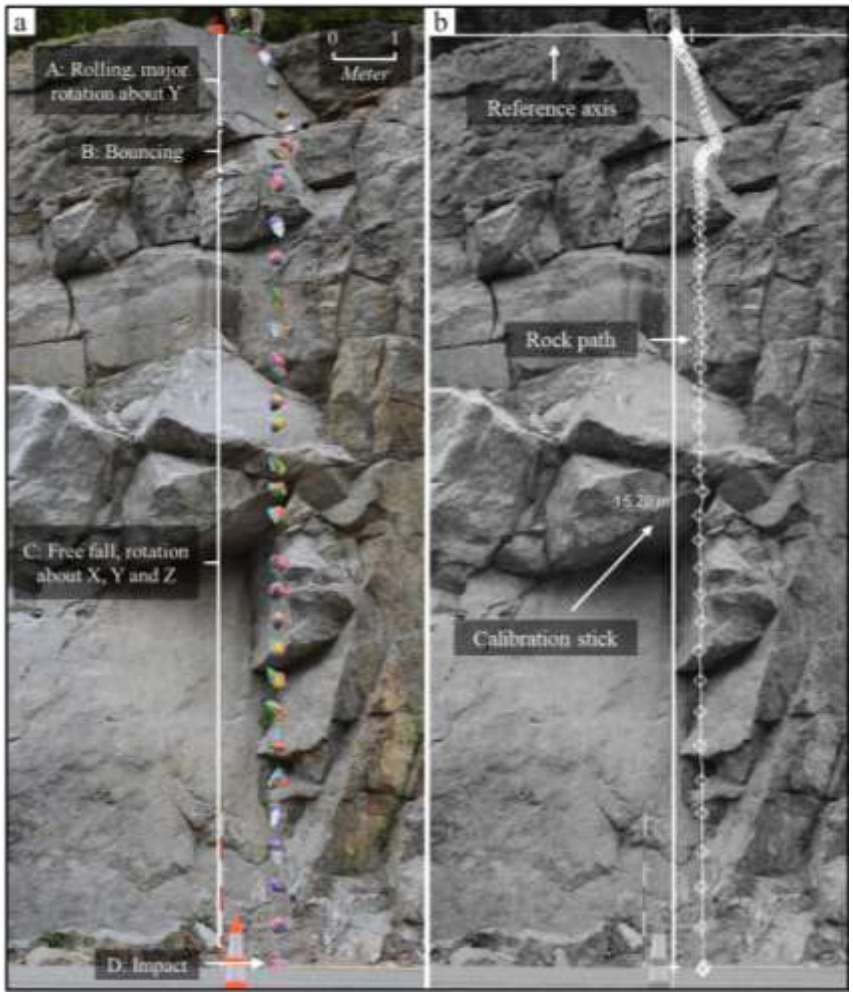

Figure 5. Rockfall trajectory for rock 6, Warner, NH: (a) combination of video frames, and (b) tracker software. The calibration of each video analysis was based on the known drop heights, measured with a total station.

For better interpretation, the three-axis acceleration and rotational velocity data were combined into resultant data plots. The test block experienced impact resultant accelerations that varied from 50 to 100 g (bouncing) to 382 g upon impact with the ground. These respective g-forces can be converted to 9 to 18 kN and 68 kN intensities, which are equivalent to approximately 1 to 2 tons forces and 7 tons force. It is important to enhance that acceleration sensors do not necessarily report accelerations and decelerations as positive and negative values, respectively. The positive or negative signal associated with accelerometer measurements are related to the sensor position at the moment / direction of impact.

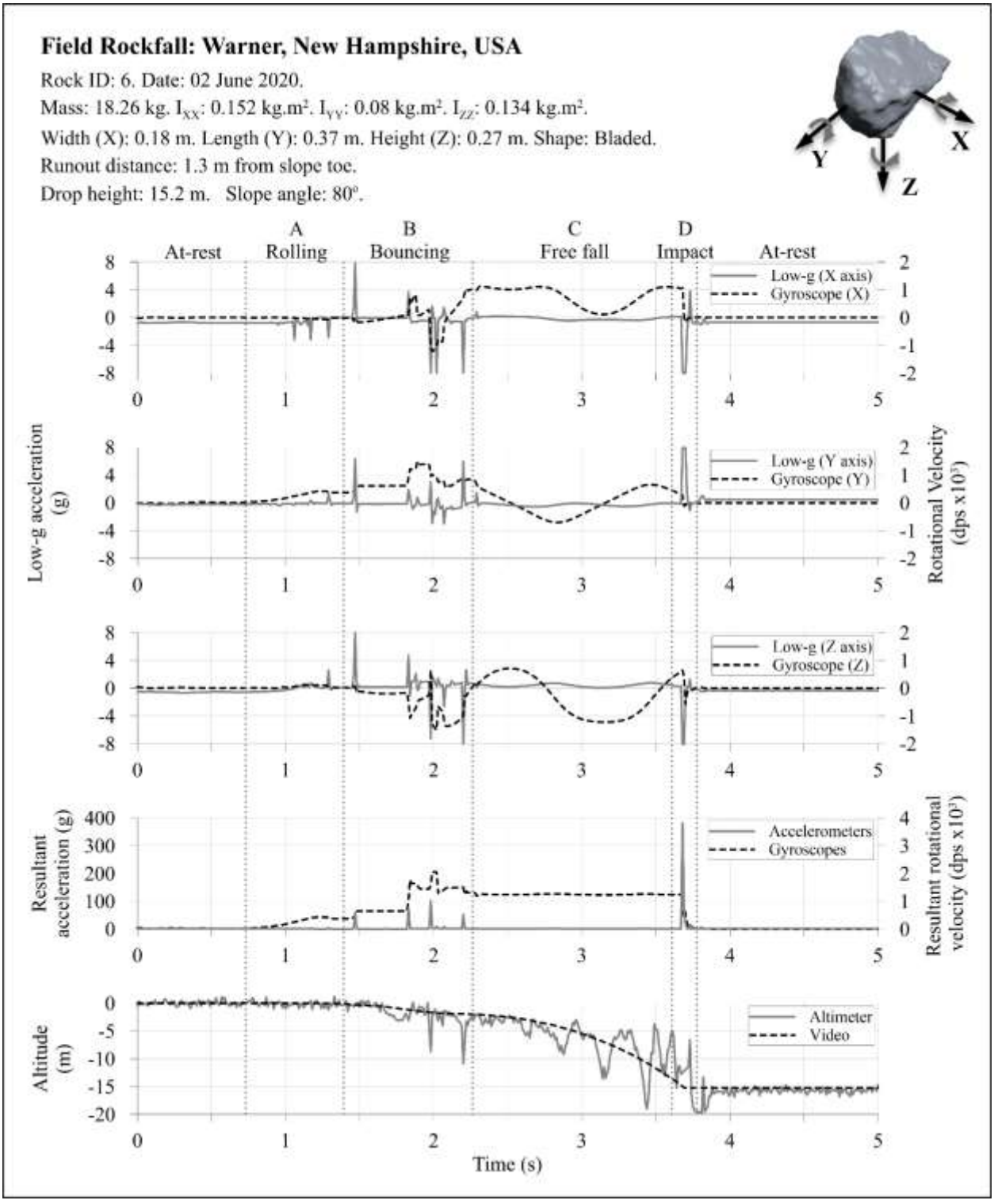

Figure 6. Rockfall trajectory for rock 6, Warner, NH: (a) combination of video frames, and (b) tracker software.

The validity of the resultant rotation data could be verified through the free fall measurements in all drop tests, which presented constant resultant rotational velocities until impact. Such behavior is accurate with Newtonian rockfall physics, as no external forces act on the rock during free fall (Turner and Duffy, 2012). In addition, it was verified that the video tracking measurements were compatible with the altitude sensor, whose data were helpful in precisely identifying the time intervals of the rockfall experiments.

From these experiments, it was possible to verify that accelerometers and gyroscopes embedded in released blocks help identify block motion as free fall, bouncing, rolling, and sliding. Their exact times can be determined through the sensor output, generally without the need for video recordings. The SR data output patterns to distinguish rockfall motion were consistent for most experimental trials, as described below. In addition, the altimeter measurements could be verified with video analysis and are presented as a promising tool for rockfall analyses where video tracking is not feasible, especially to identify the moment of ground contact.

- At-rest: zero rotational velocity, constant 1 g acceleration,
- Free fall: 0 g acceleration, constant resultant rotational velocity, the rock is free to rotate in all three directions, and the gyroscope graphs are smooth lines without peaks,
- Rolling: changes in rotational velocity accompanied by small peaks in acceleration (which typically do not exceed the capacity of the low-g accelerometer, < 8 g),
- Sliding: small acceleration peaks (which usually do not exceed the low-g sensor limits, < 8 g) accompanied by zero or small rotational velocities,
- Impact: sharp rise in acceleration, typically captured by the high-g accelerometer, which can be followed by additional impacts, rolling, sliding, or a complete stop (at-rest), and

- Bouncing: one or more impacts, followed by free fall, typically captured by the high-g accelerometer, followed by visible rotational velocity changes.

Table 2 summarizes the Smart Rock data measured in the hand-carried and scaled blocks. In general, accelerations and rotations experienced by the smaller test blocks were significantly higher than for the tests with SRs drilled in place.

Table 2. Test data summary at the ten different slope locations.

Location and avg. block weight	**Slope angles and heights**	**Smart Rock resultant data**									**Max. impact force (kN)**		
		Max. acceleration (g)			**Max. rotational vel. (dps)**			**Avg. rotational vel. (dps)**					
		Min	**Max**	**Avg**	**Min**	**Max**	**Avg**	**Min**	**Max**	**Avg**	**Min**	**Max**	**Avg**
All slopes 10 kg	25 to 90 degrees 10 to 20 meters	33	504	143	808	5396	2694	219	1935	906	2	68	13
Scaled rocks* 6000 kg	10 meters 90 degrees	17	148	59	189	3292	1025	60	200	129	1000	4800	14000
* Estimated impact force values, based on the estimated block masses													

3.2. Rockfall trajectories

This experimental campaign demonstrated that rockfall behavior can vary under different, or even similar, slope conditions. The presence of slope irregularities, commonly called launch features, potentially affects rockfall trajectories by increasing lateral dispersion, runout distances, and consequently rockfall unpredictability.

The concept of rock runout has multiple definitions in the literature and is widely used by transportation agencies to address the risks of hazards associated with rockfalls. This report refers to runout as the orthogonal distance between the toe of the rock cut and the block end location after rockfall. In addition, lateral dispersion is an important parameter to characterize rockfall

propagation. It is defined as the ratio of the block horizontal displacement (D), divided by the slope length (L), measured along the slope profile (Azzoni and de Freitas, 1995).

Figure 7 presents a histogram with ranges of lateral dispersion estimated for the slopes evaluated in this research. Measurements from video tracking have demonstrated that nearly 80% of the tested rocks came to a complete stop with lateral displacements between 0 to 20% of the slope length. These ranges agree with previous observations from Azzoni and de Freitas (1995), in which the (D/L) ratios of 60 rockfalls on 9 sites primarily varied between 10 and 20%, except for one site where the rockfall lateral dispersion was equal to 1%.

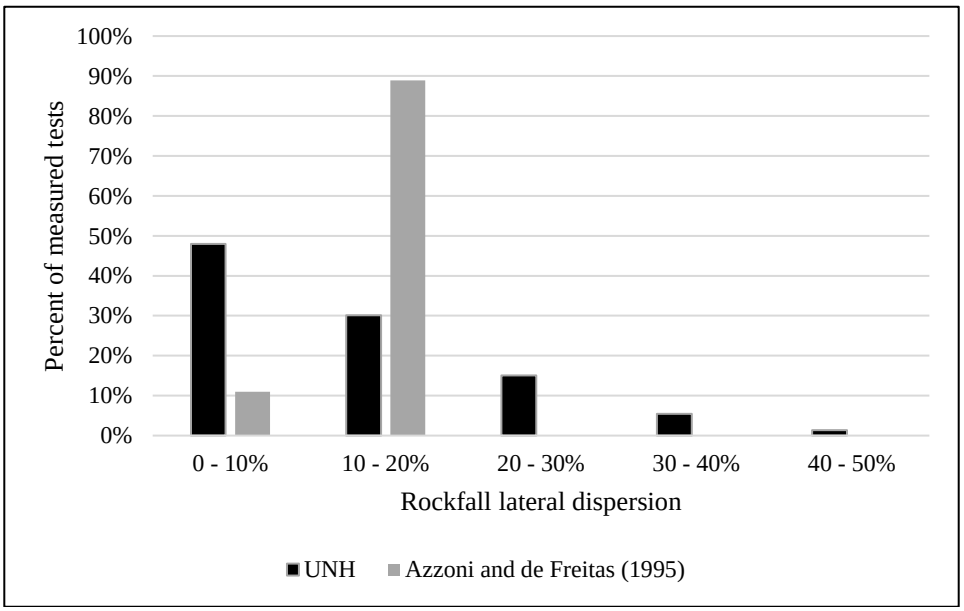

Figure 7. Histograms with lateral dispersions for experimental rockfalls in NH and VT, compared to measurements from Azzoni and de Freitas (1995). Results to the right of "0-10%" represent increasing block dispersions.

While lighter blocks had a higher ability to displace laterally, it was observed that lateral dispersion and runout were controlled mainly by the slope geometry and catchment ditch conditions. In general, rocks dropped from taller and steeper slopes described lower lateral dispersions compared to less inclined slopes and/or launch features along the rock path. Bouncing behavior on shallower slopes and slope irregularities (and consequent increases in rotational

velocity) have also typically increased rock runout. The described paths for selected sites are shown in Figure 8, which presents three steeper (slope angle > 60º) and three shallower slopes (slope angle < 60º). The trajectories on the right of Figure 9(d) occur on a 70º slope.

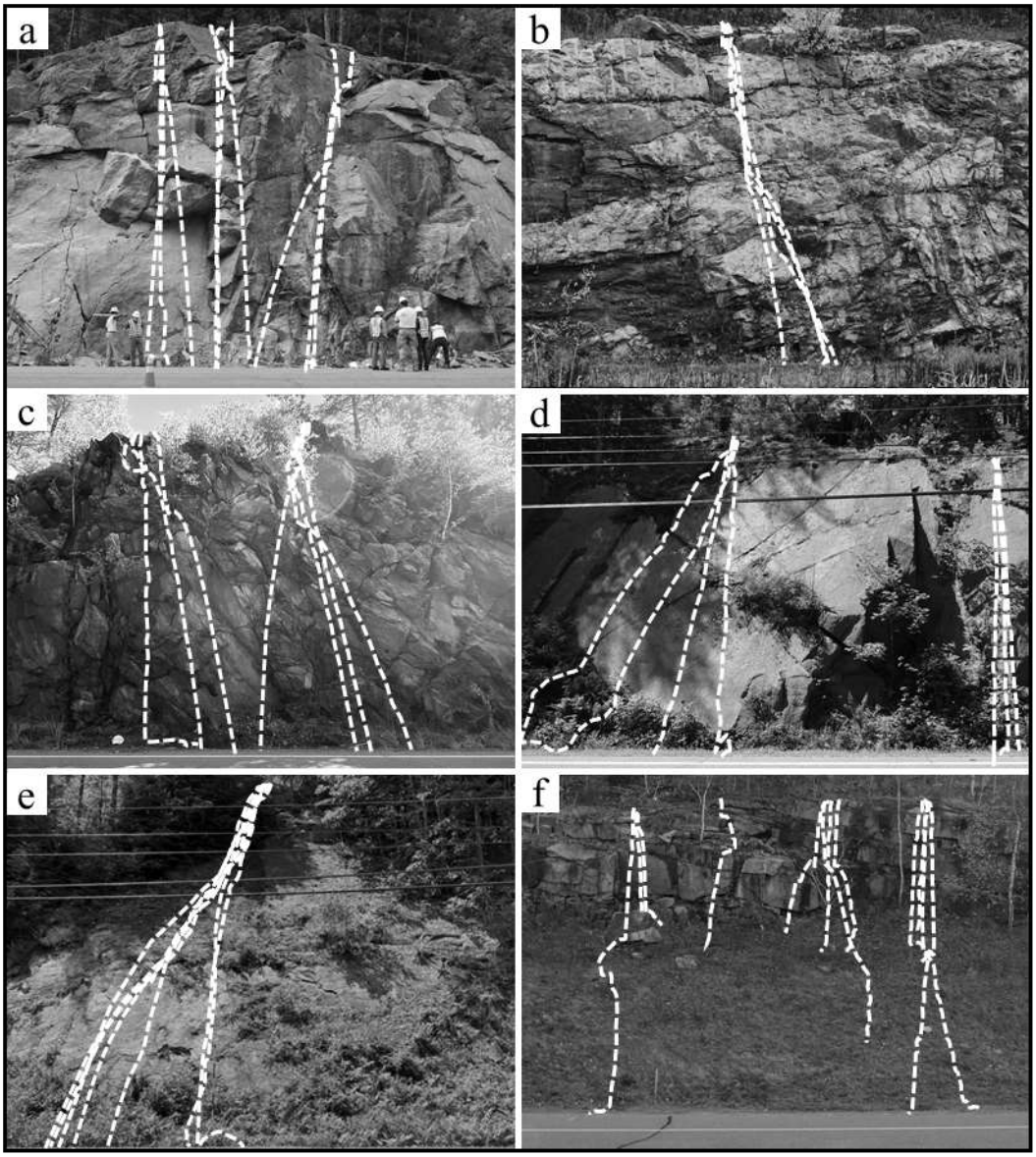

Figure 8. Rockfall trajectories in steeper slopes (a – Warner/NH, b – Windham/NH, c – Franklin 1/NH) and shallower slopes (d – Franklin 2/NH, e – Franklin 3/NH, f – Franconia/NH).

Finally, after each test, field measurements of runout distances were used to evaluate the effectiveness of catchment ditch systems under different slope conditions. Table 3 displays the

RHRS rating and runout measurements for each site, along with the characteristics and effectiveness of their respective catchment ditches. The "ditch effectiveness" score represents the percentage of rocks that have not reached the road in a given location. The most concerning rock cuts were those with shallow slopes and narrow catchment ditches.

The experiments have shown that most A-rated cuts were not fully effective in preventing rockfalls from reaching the road, while the B- and C-rated slopes successfully mitigated rockfall hazards. In addition, a correlation with the observed increase in rotation at less steep slopes can also be established between the low efficiency of certain road catchment ditches.

Table 3. Catchment ditch characteristics for each site and measured runout distances.

Site/ Slope angle	**Rating**	**Catchment ditch**			**Runout (m)**				**Ditch effectiveness**
		Material	**Width (m)**	**Geometry**	**Min.**	**Max.**	**Avg.**	**Stdev.**	
Townshend, VT 30º to 80º	A	Talus	2.5	Irregular downward	0.0	6.6	2.8	2.9	67%
Warner, NH 70º to 85º	A	Soil	3.5 to 5.0	Flat	0.0	4.3	1.7	0.9	100%
Franklin 1, NH 45º to 90º	A	Soil covered with grass	1.3	Flat	0.0	10.6	3.5	3.8	38%
Franklin 2, NH 50º to 70º	A	Soil covered with grass	2.5	Trapezoidal	0.2	3.5	1.9	1.1	57%
Franklin 3, NH 40º	A	Soil covered with grass	3.0	Trapezoidal	0.2	7.6	3.6	1.8	43%
Danbury, NH 70º to 75º	A	Soil covered with grass	2.0	Flat	0.3	4.1	1.6	1.2	78%
Windham, NH 60º to 65º	B	Talus	2.0	Trapezoidal	1.7	4.4	3.3	1.2	N/A*
Orange, NH 65º to 75º	B	Soil covered with grass	5.0	Flat	1.5	3.4	2.1	0.6	100%
Franconia, NH 25º to 90º	B	Grass / soil	10.0 / 1.5	25º / Flat	0.0	10.5	4.6	4.0	100%
Keene, NH 70º to 75º	C	Soil	-	Flat	0.0	3.9	2.2	1.3	N/A*

* Not located near transportation corridors.

4. DISCUSSION OF FIELD RESULTS

4.1. Rockfall measurements with the Smart Rock

Equation 2 addresses critical parameters associated with acceleration levels experienced by free-falling objects (Leonhardt, 2001). The acceleration of a dropped object is a function of the modulus of elasticity of the dropped object (E), the contact area of the falling rock (A), the acceleration of gravity (g), the drop height (d_1), the compression displacement of the falling rock (h), and the mass of the object (m).

$$a = \sqrt{\frac{E\ A\ g\ d_1}{h\ m}} \qquad \text{(Equation 2)}$$

From Equation 2, there are different circumstances in which greater acceleration levels can be achieved. Therefore, higher accelerations are expected:

- When the surface area (A) is increased – impacts on a flat face of an object will experience a higher acceleration than if the impact occurs on a sharp corner,
- At higher drop heights (d_1),
- With lower mass objects (m), and
- With stiffer objects (higher modulus E) and harder impact surfaces (lower compression h).

Therefore, objects dropped onto rigid and less deformable surfaces can achieve remarkably high levels of acceleration. In this research, higher acceleration was measured upon impacts on rock, compared to other less stiff materials such as granular soil, covered with or without grass. In addition, rocks of lower mass and/or released from higher drop heights have, in general, experienced higher acceleration magnitudes. Most peak accelerations experienced by the smaller test blocks are significantly higher than for the tests with rocks drilled in place, whose average of the peak accelerations was equal to 66 g.

Coupled with the accelerometer data, the measured rotational velocities in a rockfall experiment can be used to readily identify changes in rock motion, especially during bouncing and free-falling periods, through constant resultant rotation or abrupt changes in rotational motion, respectively. Figure 9 presents the maximum and average resultant rotational velocities experienced for each test, plotted against the mass of the released blocks. The Smart Rock data have demonstrated that, in general, blocks of smaller mass (and smaller moments of inertia) are more easily subjected to changes in rotation for the same drop height. This behavior can be associated with the difficulty in rotating blocks with higher mass (higher moments of inertia) for shorter slopes normally encountered in New Hampshire.

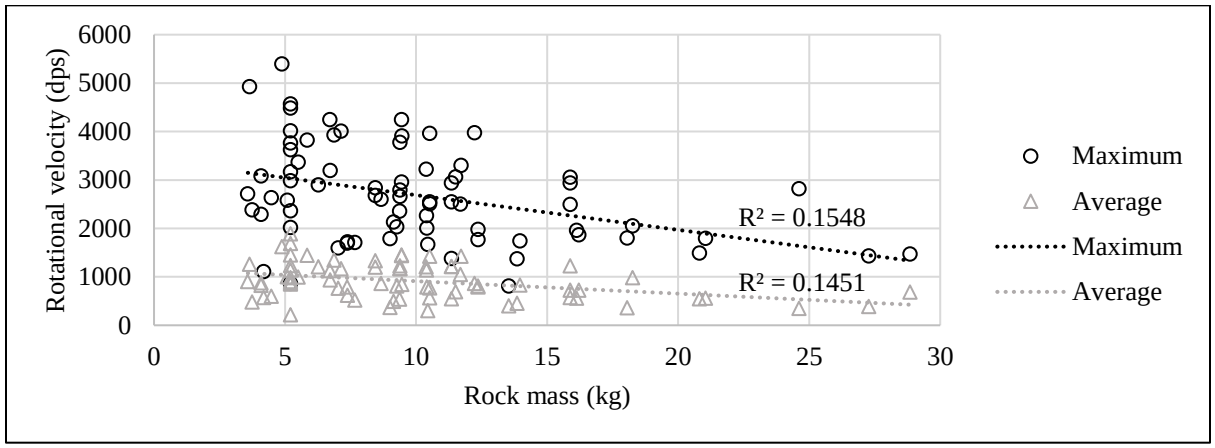

Figure 9. Maximum and average resultant rotational velocities for the 11 test sites as a function of block mass.

4.2. Identified rockfall motion and measured block displacements

The SR can also be used to precisely identify different modes of motion experienced during the entire fall. The measured acceleration and rotational velocity outputs from these experiments are the first steps to validate and improve rockfall computational models and ultimately help with mitigation methods.

Output patterns in the sensor signal were used to identify whether falling blocks described free fall, rolling, bouncing, or sliding behaviors at different slope positions and configurations.

This information was compared to the research report written by Ritchie (1963) used to define practical ditch design criteria based on slope height, slope angle, and catchment area depth. It was observed that rockfall motion type is strongly influenced by the slope angle, identifying specific ranges at which a particular behavior usually governs. He stated that blocks tend to roll on slopes up to 45º, bounce between 46º and 63º, and fall freely for surface inclinations higher than 63º.

Therefore, predominant rockfall motion identified at different ranges of slope angle in this research is presented in Table 4. In general, prevalent rolling behavior during rockfall was mainly observed at the beginning of most tests and on soil slopes covered with vegetation.

The observations for each site were grouped by ranges of slope angle (Figure 10), similar to Ritchie's study. It was observed that test rocks of distinct shapes and sizes tended to roll/bounce on slopes between 20º and 30º and bounce on slopes between 40º and 60º. Furthermore, a transition zone between bouncing and free fall behavior was identified for slopes between 60º and 65º, and slopes between 65º and 90º led the falling blocks to mostly fall freely. Therefore, the described rockfall behavior was compatible with previous conclusions from Ritchie (1963), suggesting that the Smart Rock sensor was an effective tool to identify rockfall modes of motion accurately.

Finally, as the rock falls along the slope profile, the following sequence was typically observed in this research:

1. Rolling and/or sliding,
2. Bouncing (at slope profiles with inclinations lower to 65º),
3. Free fall with bouncing against launch features (at slope profiles steeper than 60º), and
4. Bouncing against the ground surface, followed by additional bounces or subsequent rolling motion until a complete stop.

Table 4. Predominant rockfall behavior at each site.

Site	Surface inclination	Predominant motion	Remarks
Dover, NH	50º to 60º*	Bouncing	Significant surface roughness and rock mass discontinuities
Danbury, NH	20º	Bouncing / Rolling	Soil covered with grass and leaves
	70º to 75º	Free fall	Isolated bounces on launch features
Franconia, NH	25º to 30º	Bouncing / Rolling	Grass slope
	50º to 65º	Bouncing	Slope cross-section formed by "steps"
	65º to 90º	Free fall	Bounces on launch features
Franklin 1, NH	45º	Bouncing	Early stages of rockfall, upper portion of the slope
	80º to 90º	Free fall	Isolated bounces on launch features
Franklin 2, NH	50º	Bouncing	Free fall from the middle to the slope bottom, at higher velocities
	70º	Free fall	Rolling/bouncing only on the upper portion of the slope
Franklin 3, NH	40º	Bouncing	Slope with a most significant bouncing motion
Keene, NH	70º to 75º	Free fall	Blocks usually bounced one time
Orange, NH	65º	Free fall / Bouncing	Early stages of rockfall, upper portion of the slope
	75º	Free fall	
Townshend, VT	30º	Bouncing	Abrupt change of surface angle in the middle of the slope profile
	80º	Free fall	
Warner, NH	45º	Bouncing	Early stages of rockfall, upper portion of the slope
	70º to 85º	Free fall	Bounces on launch features
Windham, NH	60º to 65º	Free fall / Bouncing	One or two bounces on the rock face

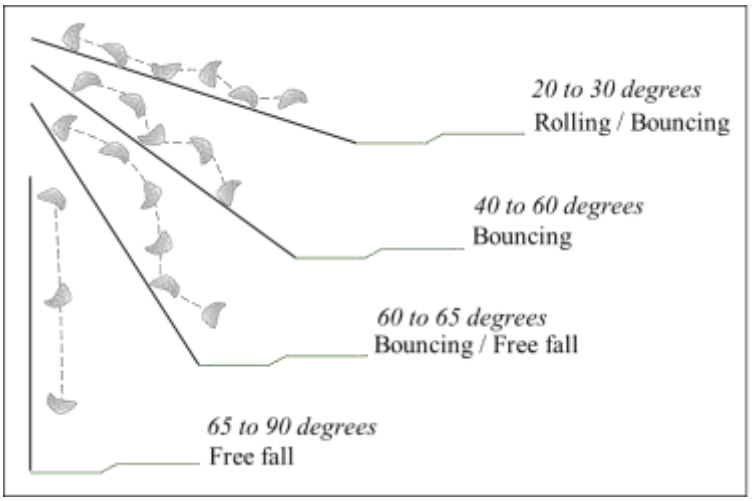

Figure 10. Rockfall modes of motion for different slope angles.

Runout distances were potentially increased in test sites where rolling and/or bouncing motion occurred after ground contact, as Pierson (2001) observed. However, a small number of tests completely stopped immediately after impact, demonstrating a complete kinetic energy dissipation, especially on loose/soft ground. Therefore, shorter post-impact displacements and runout distances occurred when the test blocks impacted against catchment ditches formed by granular soil, as Ritchie (1963) noted. On the other hand, longer runouts were observed after impact on stiffer ground surfaces (e.g., pavement, talus ditches).

Ritchie (1963) and Pierson et al. (2001) argued that runout distances could potentially increase when blocks predominantly bounce. Therefore, the presence of launch features and shallower slope angles pose a safety concern in areas with narrow catchment ditches and/or a lack of protective structures. Longer runout after impacts on slope irregularities was observed in slopes in Franklin 1, Danbury, and Townshend, where blocks reached the road. In addition, besides aspects related to the rock face geometry, significant dispersion of the measured runouts was also attributed to the flat or descending geometry of the catchment ditch in most test locations.

Although significant bounce heights after ground impact were not observed in the field trials, 25% of the rockfall tests near transportation corridors reached the road. This behavior occurred especially in all three Franklin slopes. In general, rockfalls on slopes between 40° and 50º caused the test blocks to develop higher horizontal velocities and more significant runouts due to the bouncing behavior on these inclined surfaces during a rockfall. According to Ritchie (1963), less inclined surfaces near 45º are more concerning in rockfall risk mitigation, as they create higher lateral and rotational motion conditions.

4.3. Summary of findings

The Smart Rock data and field measurements acquired in this experimental campaign yielded the general observations presented in Table 5. Although general trends could be observed, data variability is still significant and numerical relationships could not be established for rockfall influencing parameters. Further assessments of isolated parameters are still necessary to quantify any possible correlations.

Table 5. General observations of rockfall behavior during the experimental campaign.

Change in parameter	**Acceleration**	**Impact force**	**Block rotation**	**Lateral dispersion**	**Runout distance**
Increase block mass	↓ Decreases	↑ Increases	↓ Decreases	× Correlation not established	× Correlation not established
Decrease slope angle	↑ Increases	↑ Increases	↑ Increases	↑ Increases	↑ Increases
Increase slope height	↑ Increases	↑ Increases	× Correlation not established	× Correlation not established	× Correlation not established
Increase in block rotation	× Correlation not established	× Correlation not established	-	↑ Increases	↑ Increases
Presence of launch features in the rock face	↑ Increases	↑ Increases	↑ Increases	↑ Increases	↑ Increases
Impacts on stiffer ground surface/ditch	↑ Increases	↑ Increases	↓ Decreases	↑ Increases	↑ Increases

4.4. Review of design charts

The observations from Ritchie's study (1963) were used as recommendations for the design of catchment ditches based only on the height and angle of the rock slope (Figure 11). These recommendations have been used as design guides for catchment ditches for more than 50 years, and have been revised and expanded by Pierson et al. (2001), who have provided design charts to estimate percentages of retained rockfalls considering different slope heights and catchment ditch conditions, such as widths and gradients (Figure 12).

The field assessments performed in this research included performing experimental rockfalls, measuring rock distances traveled, and measuring the slope height and catchment ditch (width and depth) of each site location. The obtained information was compared to the design charts prepared by Ritchie (1963) and Pierson et al. (2001), commonly used in rockfall design in the United States.

The design charts presented in Figures 11 and 12 include measurements performed at the Danbury site (10.5 m – 34ft – tall cut, 70° to 75° slope – 3V:1H). For the given slope conditions, Richie's chart (Figure 11) recommends a 15-foot (4.6 m) wide and 5-foot (1.5 m) deep catchment ditch. The site conditions, however, consist of a 2.0 m wide, 0.3 m tall (1V:7H gradient) catchment ditch due to the lack of space between the slope and the road.

The percent rockfall retained design charts proposed by Pierson et al. (2001) consider different ranges of slope heights (12, 15, 18, and 21 m) and gradients equivalent to the slope angle (vertical, 4V:1H, 2V:1H, 1.33V:1H, 1V:1H). In this assessment, the nearest higher chart slope height compared to the field measurement was used at each location (e.g., 12 m chart for a 10 m slope), and interpolation between charts was performed for intermediate slope gradients. Thus, the lack of specific design charts for each slope configuration can overestimate rockfall trajectories. For the Danbury site, Pierson et al.'s charts for 12 m tall slopes with 4V:1H and 2V:1H gradients were used, and their results were interpolated.

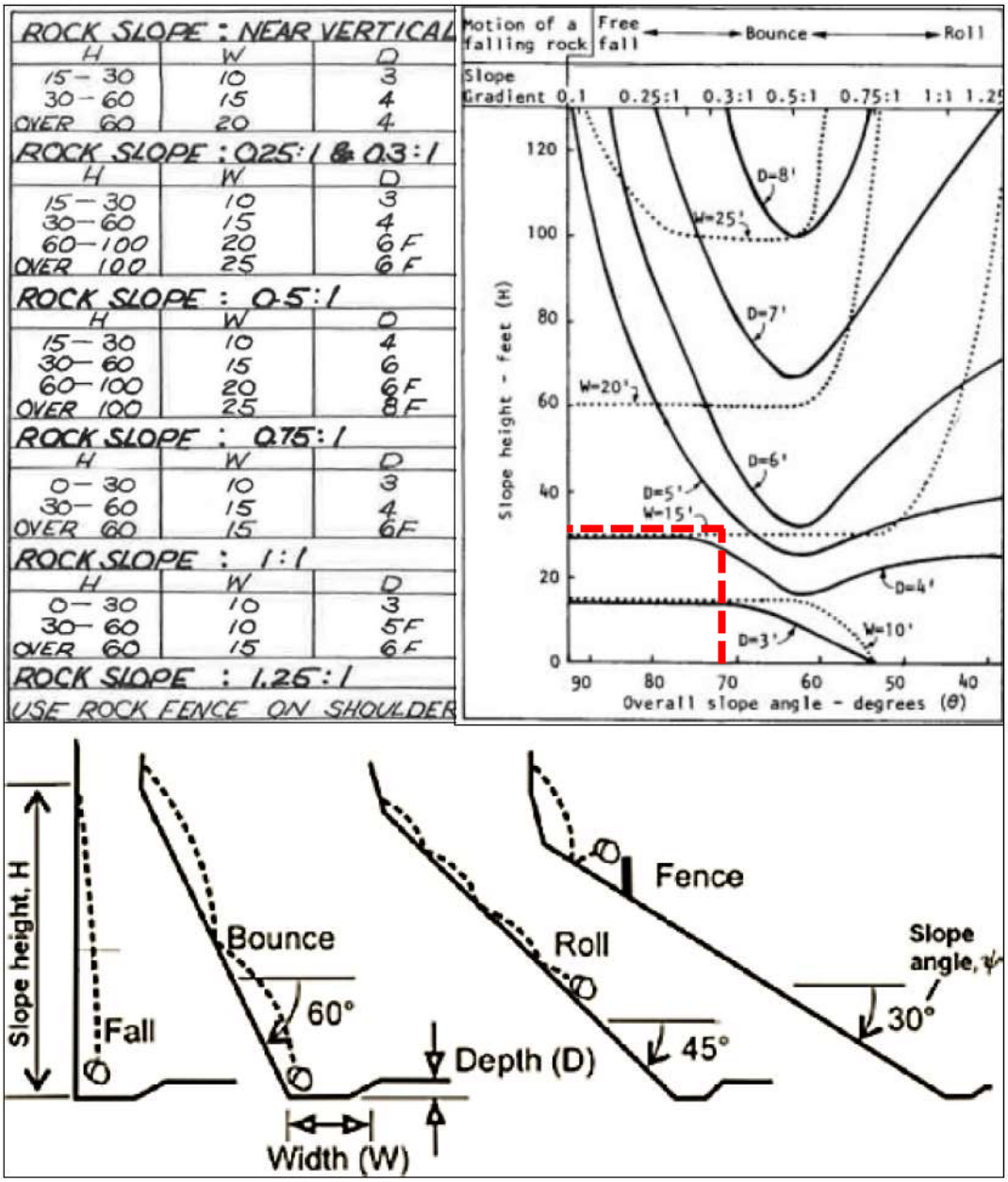

Figure 11. Catchment ditch design chart by Ritchie (1963). The dashed lines indicate the slope conditions in Danbury, NH.

Figure 12 suggests that approximately 30% of rockfalls are retained for 12 m slopes with a 2V:1H gradient. This estimate was interpolated with approximately 70% of retained rockfalls for a 4V:1H gradient, resulting in an overall estimate of 55% of retained rockfalls. This prediction is conservative considering the field measurements, where 78% of the rockfalls did not reach the

road. It is important to highlight that the design charts developed by Pierson et al. (2001) should consider the existing catchment ditch dimensions (on site), instead of the depth (D) and width (W) values recommended by Ritchie's chart.

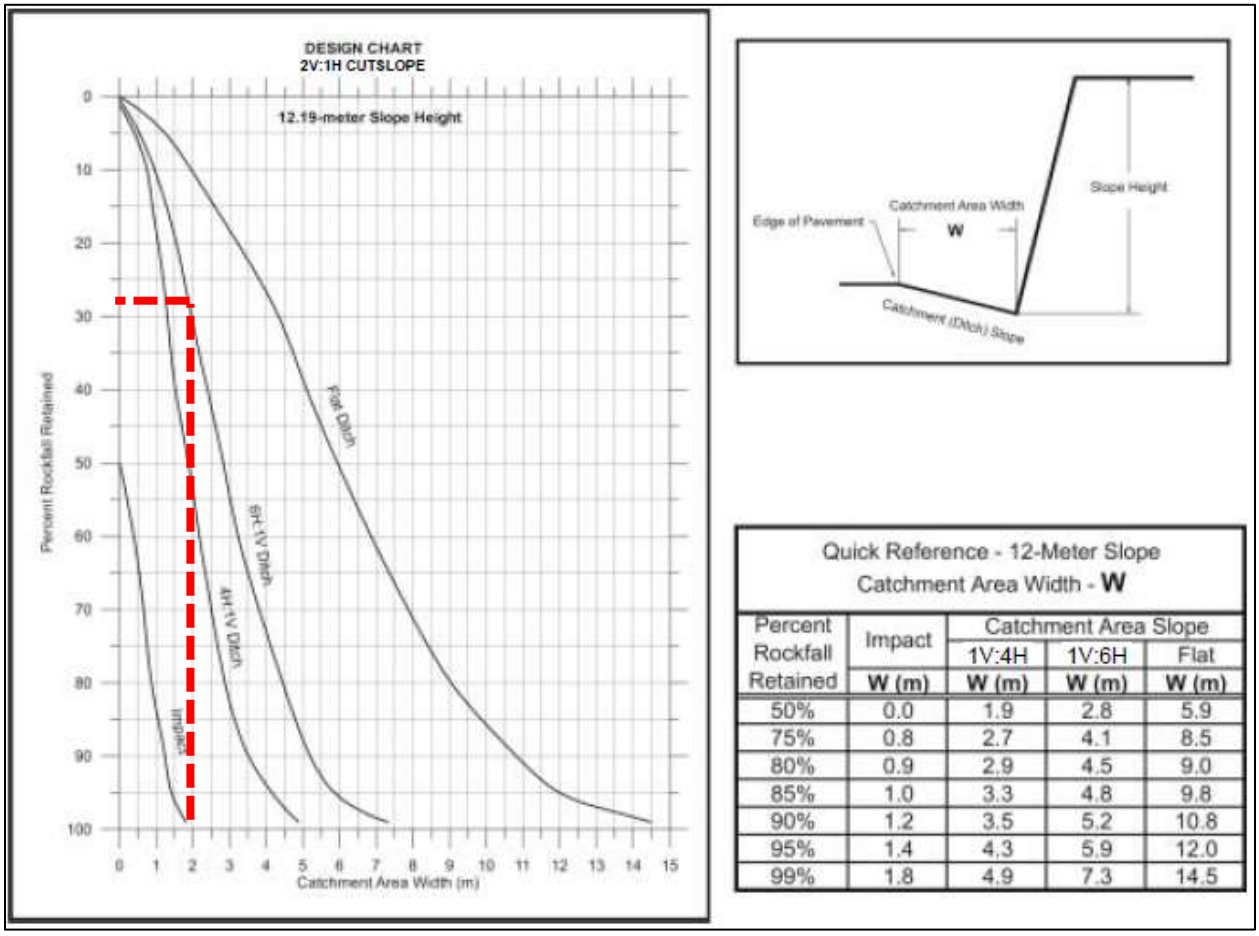

Quick Reference - 12-Meter Slope
Catchment Area Width - **W**

Percent Rockfall Retained	Impact	Catchment Area Slope		
		1V:4H	1V:6H	Flat
	W (m)	W (m)	W (m)	W (m)
50%	0.0	1.9	2.8	5.9
75%	0.8	2.7	4.1	8.5
80%	0.9	2.9	4.5	9.0
85%	1.0	3.3	4.8	9.8
90%	1.2	3.5	5.2	10.8
95%	1.4	4.3	5.9	12.0
99%	1.8	4.9	7.3	14.5

Figure 12. Sample design chart by Pierson et al. (2001) for a 12 m rock cut with a 2V:1H gradient. The dashed lines indicate the slope conditions in Danbury, NH.

Table 6 presents a summary of the recommendations of both design charts for each New Hampshire site. The rock cut in Vermont was not included in these estimates, since the catchment ditch was covered by rock talus due to ongoing scaling work. Thus, ditch measurements could not be performed at this site.

In general, both sets of design charts were overconservative to predict the necessary catchment ditch dimensions in order to contain all rockfalls. While the results obtained by Ritchie's charts suggest that significantly superior dimensions are needed for the catchment ditch than the current field conditions, it was often not possible to follow these recommendations due to the restricted available space between the rock cut and the road. On the other hand, even though most catchment ditch size recommendations could not be followed, the percent of retained rockfalls estimated by the Pierson et al. charts for the existing site conditions were also significantly inferior to the measured field behavior.

Table 6. Summary of review of design charts.

ON-SITE CONDITIONS							DESIGN CHARTS		
Slope ID	Slope height	Slope angle	Catchment ditch			Rockfall retained	Ritchie		Pierson
			Depth D	Width W	Gradient		Depth D	Width W	Rockfall retained
Danbury	10.5 m 34 ft	70º to 75º 3V:1H	0.3 m 1.0 ft	2.0 m 6.6 ft	10° 1V:7H	78%	1.5 m 5.0 ft	4.6 m 15 ft	55%
Franconia	4.0 m 13 ft	90°	5.5 m 18 ft	10 m 33 ft	30° 1V:2H*	100%	***	***	***
Franklin 1	12.5 m 41 ft	90º	0.1 m 0.3 ft	1.3 m 4.3 ft	5° Flat	38%	1.5 m 5.0 ft	5.2 m 17 ft	35%
Franklin 2	10.0 m 33 ft	50° 1V:1H	0.15 m 0.5 ft	2.5 m 8.2 ft	5° Flat	25%	1.5 m 5.0 ft	4.6 m 15 ft	10%
Franklin 2	8.0 m 26 ft	70° 3V:1H	0.15 m 0.5 ft	2.5 m 8.2 ft	5° Flat	67%	1.2 m 4.0 ft	4.6 m 15 ft	40%
Franklin 3	18 m 60 ft	40º 1V:1H	0.15 m 0.5 ft	2.5 m 8.2 ft	5° Flat	43%	1.8 m 6.0 ft	4.6 m 15 ft	10%
Keene	10.0 m 33 ft	70º to 75º 3V:1H	0.0 m 0.0 ft	**	Flat	**	1.5 m 5.0 ft	4.6 m 15 ft	**
Orange	9.0 m 30 ft	65º to 75º 3V:1H	0.3 m 1.0 ft	5.0 m 16 ft	5° Flat	100%	1.5 m 5.0 ft	4.6 m 15 ft	65%
Warner	15.0 m 50 ft	70º to 85º 4V:1H	0.0 m 0.0 ft	4.0 m 13 ft	Flat	100%	1.8 m 6.0 ft	6.1 m 20 ft	90%
Windham	12.5 m 41 ft	60º to 65º 2V:1H	0.0 m 0.0 ft	**	Flat	**	2.1 m 7.0 ft	6.1 m 20 ft	**

* Downward towards the road

** The slope was not located near transportation corridors, and the catchment ditch was infinitely long

*** Slope conditions were not compatible with design charts due to both slope height and ditch geometry

5. LABORATORY EXPERIMENTS

Rockfall trajectories are typically simulated through computational modeling to assist in the design of protective structures. However, the uncertainty related to rockfall behavior and model input parameters is still significantly high. Rock bouncing motion occurs when falling blocks impact the rock slope or other surfaces (sand, grass, gravel, asphalt). Although the rebound behavior depends on block characteristics (shape, weight, and size) and the impact surface, the rebound behavior is mathematically governed by one or two coefficients calculated from normal and tangential velocity ratios after and before impact, designated as coefficients of restitution (COR_N and COR_T). Table 7 presents ranges of normal coefficients of restitution (COR_N) observed for typical impact surfaces. The tangential coefficients of restitution (COR_T) are often optional components in rockfall modeling, since it is not always possible to estimate tangential velocities before impact (when blocks are released perpendicularly against flat surfaces, as performed in this research).

Table 7. Typical ranges of COR_N used in rockfall modeling.

Source	**Rock**	**Soil**	**Rock talus**
Default (Rocscience)	0.35	0.30	0.32
Literature	0.12 to 0.88 Peng (2000) Asteriou et al. (2012)	0.10 to 0.32 Peng (2000) Pfeiffer and Bowen (1989)*	0.07 to 0.45 Peng (2000) Heierli (1985)*
* Cited by Heidenreich (2004)			

In this research, a preliminary instrumented small-scale experimental campaign was conducted to evaluate coefficients of restitution on granular material and rock. The obtained COR values were used as model input parameters in two-dimensional rockfall simulations and compared to trajectories obtained from default coefficients. Both models were compared to trajectories measured in field experiments conducted at a 15 m tall, high-hazard rock cut in Warner, NH.

5.1. Laboratory methodology

Energy restitution experiments were carried out in a test pit in the UNH Geotechnical Laboratory. A Kinsman Granodiorite test rock from Warner/NH was initially cut into a cubic block of approximately 1 kg. In a second round of tests, the block edges were cut, resulting on a cuboctahedron of 0.8 kg. The results were used to evaluate how rock kinematics during and after impact were affected by shape alteration. The test blocks had a 25.4 mm diameter hole, drilled for the Smart Rock sensor, as previously performed in the field trials.

The test block was consistently dropped from a drop device with a trap door mechanism, which allowed the test block to fall with no rotation motion. The box height can be freely adjusted within the frame, allowing tests to be conducted consistently with different drop heights. For these tests, the rock dropper was set up at a constant drop height of 2.2 meters.

The first tests were conducted on a 50 cm layer of fine sand, compacted using a jackhammer tamper. Ten drop tests from a 90º release angle on the flat, granular material surface were conducted for each test block geometry. After each test, the maximum embedment depth was measured with a caliper, and the test surface was leveled and prepared for the subsequent trial. In a second stage, three tests were performed by dropping the cuboctahedron from 2.2 m on a 60 cm x 30 cm x 15 cm Kinsman Granodiorite also retrieved at the Warner site, embedded in plaster for a precise adjustment of the surface angle at 0º.

Each experiment was recorded with a frontal (240 fps) and an upper camera (120 fps). The velocities of the released block were estimated through Tracker 5.1.5 software. The tests were instrumented with Smart Rocks at a sampling frequency of 500 Hz, and the altimeter was disabled due to its significant data noise at high frequencies. Each test signal could be easily identified through a sharp peak in acceleration upon impact, which was used to match the sensor and video

data to the same time intervals. Finally, the estimated bounce heights, velocities, and kinetic energies from these experiments were used to calculate these coefficients.

5.2. Results and discussion

Figure 13 presents the different behavior observed for the tests on sand and on rock. The video and sensor measurements demonstrated that the cubic block, which had a larger surface contact area during impact, presented a distinct behavior from the cuboctahedron when dropped on sand. As expected, the energy restitution on rock was significantly higher.

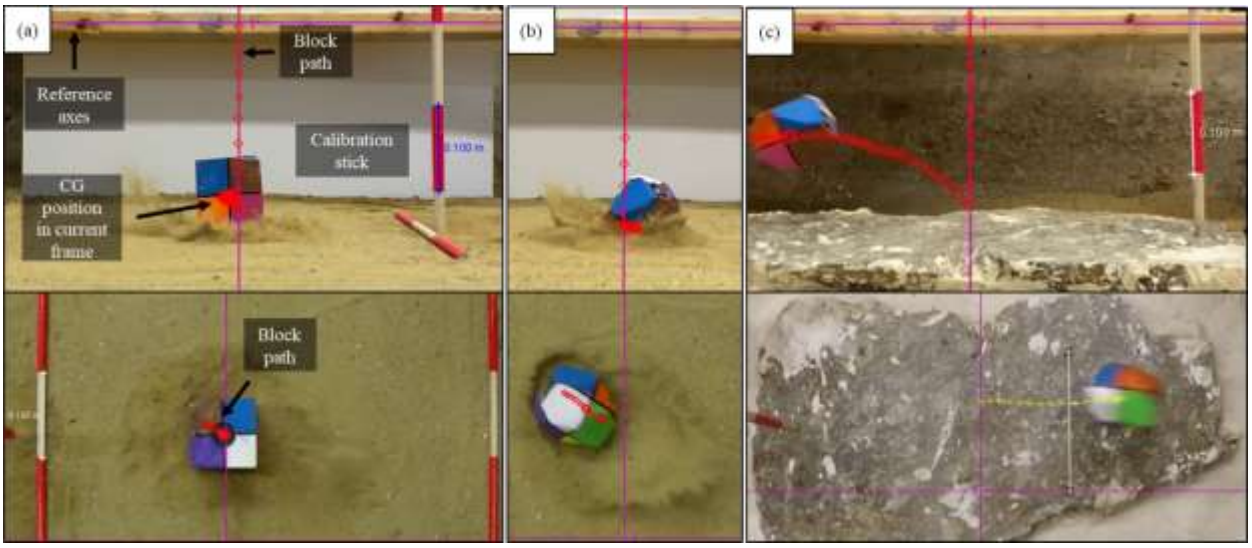

Figure 13. Block rebound against (a) sand, cubic shape, (b) sand, cuboctahedron shape, and (c) rock, cuboctahedron.

It was identified that the block penetration in the sand governs the rebound and energy restitution behavior. Higher embedment depths (ground deformation) implied higher rotation and a rolling behavior instead of block bouncing. Table 8 displays the differences in behavior observed in both samples under identical release and impact conditions on sand.

Table 8. General observations of rockfall behavior during the experimental campaign on sand.

Parameter	Flat contact area	"Rounded" contact area
Acceleration	↑ Increases	↓ Decreases
Block rotation	↓ Decreases	↑ Increases
Lateral dispersion	↓ Decreases	↑ Increases
Block embedment	↓ Decreases	↑ Increases
Block rebound	↑ Increases	↓ Decreases

Table 9 presents the calculated coefficients of restitution for each impact surface. The COR values obtained from the trials with the cubic block are within the lower limit ranges of COR published in the literature and are significantly lower than default coefficients used in two-dimensional modeling, equal to approximately 0.30. The higher energy dissipation observed with the cuboctahedron tests yielded lower COR values. However, assuming nearly zero restitution on sand slopes potentially underestimates rockfall trajectories resulting in potential increased the risk of hazards to the public.

Table 9. COR results for the drop tests performed.

Material	Average coefficients of restitution	
	COR_N (rebound measurements)	COR_N (velocity measurements)
Sand (cube)	0.08 ± 0.01	0.08 ± 0.01
Sand (cuboctahedron)	-	0.03 ± 0.02
Rock (cuboctahedron)	0.24	0.21

In addition, the COR values from both tests on rock are compatible with field and laboratory tests from previous authors. However, most of the energy assessments published in the literature present higher restitution values, including default coefficients used in modeling software. Therefore, it is a challenging task to select representative parameters for trajectory predictions and additional energy assessments are needed.

5.3. Rockfall modeling

The obtained COR values were evaluated in a digital rockfall model of a high-hazard, 15 m road cut in Warner/NH, where eight field rockfall experiments were performed with local rocks for model comparisons. The catchment ditch is 3.5 to 5 m wide, flat, and composed of granular soil.

The point cloud of the site location was obtained from the NHDOT generated by structure from motion photogrammetry. These simulations were performed using RocFall software by Rocscience, which can calculate bounce heights, energies, and velocities for 2D trajectories. The model results obtained from the laboratory coefficients were compared with models using default coefficients. The software imported the slope cross-sections as coordinates obtained from 3D surface models generated by photogrammetry by Neil Olson at the NHDOT Bureau of Materials and Research. Representative cross-sections from each field test were extracted from the 3D slope model.

Fifty rockfall simulations were performed for each test rock, whose mass, shape, and density were imported for each assessment. For more straightforward data processing in 2D, the geometry of each rock was simplified, and the release location was similar to the drop locations of the field tests.

Figure 14 presents the modeled rock shapes and trajectories for an 18 kg block. The red trajectories represent the cross-section with rotation about the axis of lowest inertia, while the green trajectories represent the cross-section that rotates about the axis of highest inertia, as represented in Figure 15. The black trajectory was approximated from the field experiment, and the block had a ground impact energy that was wholly absorbed (zero bounce height).

Compared to the field tests with the same rocks and slope cross-sections, the modeled rockfall motion type (free fall, rolling, bouncing) before ground impact typically agreed with the

field observations. However, the quantitative data (bounce heights, runout, and rotational velocities) were often overestimated, leading to overly conservative ditch geometry and protective structures. Although the laboratory-based coefficients estimated smaller bounce heights more compatible with the field behavior, the rotational motion was not significantly decreased after the first impacts with the ground as observed in the field.

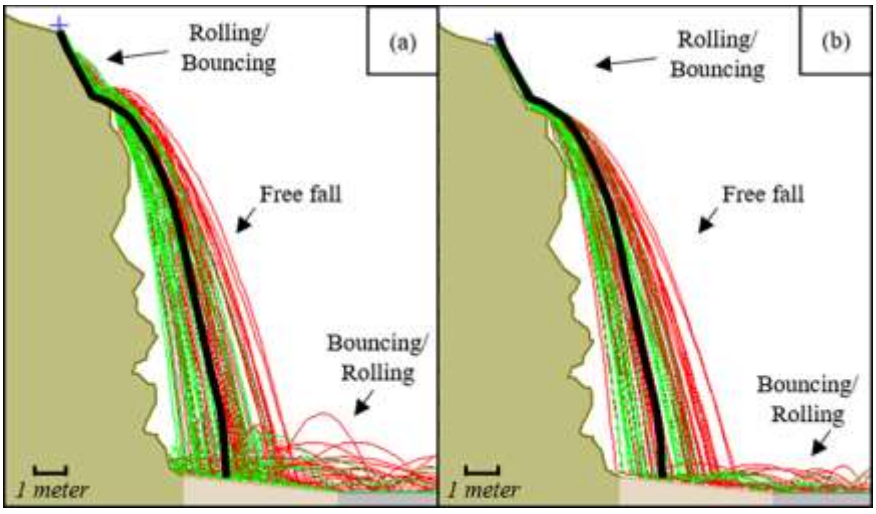

Figure 14. Rockfall models from (a) default and (b) laboratory CORs. The black trajectory represents the field test.

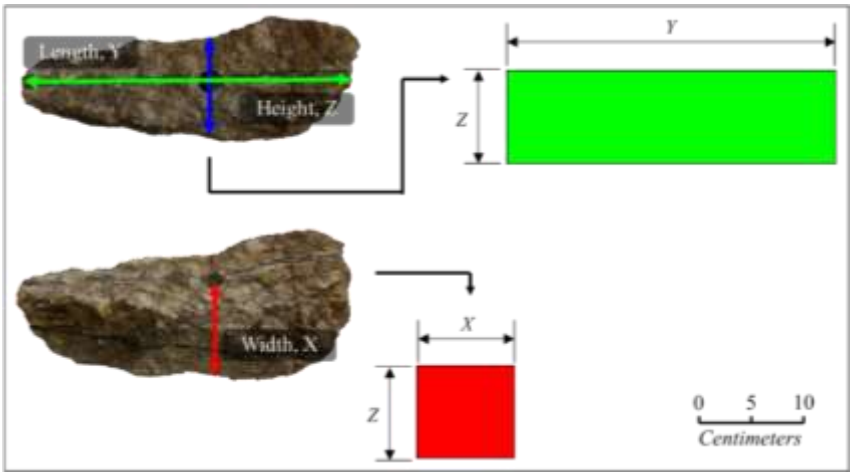

Figure 15. Cross-sections for a modeled test block from Warner/NH.

Therefore, these early results suggest that the current predictive methods were not fully compatible with the recorded data and measured runouts from the full-scale experiments. These recent models typically assume restitution and friction parameters, resulting in protective designs that can be unsafe by not properly accounting for the rotational energy, and overly conservative in terms of block displacements. There is an increasing need to estimate coefficients of restitution capable of realistically predicting the dispersion of falling rocks in typical surfaces, and the Smart Rock can be considered a promising tool for more accurate assessments and consequent hazard mitigation.

6. SUMMARY AND CONCLUSIONS

6.1. Summary

The objectives for this research were to characterize rockfall motion over time from the perspective of the falling rock and conduct preliminary laboratory and modeling assessments to evaluate two-dimensional simulated trajectories. Smart Rock sensors were used to analyze field measurements performed with several test blocks on slope profiles of different characteristics. In order to achieve these objectives, this research examined:

- How acceleration, rotation, altitude from a Smart Rock sensor can be used to characterize the motion of a falling rock, coupled with video observations.
- How the measured rockfall behavior can vary under different, or even similar, slope conditions and falling block characteristics.
- How velocity- and energy-based coefficients of restitution can be evaluated with Smart Rock data using an experimental laboratory setup.
- How trajectories, runout distances, and rotational velocities differ from the field measurements using default and laboratory-based input parameters.

A total of 85 instrumented field experiments was conducted on 10 medium-to-high hazard rock cuts in New Hampshire and one high-hazard slope in Vermont. The Smart Rock sensor was embedded in the center of gravity of natural rocks collected at each site and prepared in the laboratory. The Smart Rock data allowed more in-depth evaluations of acceleration magnitudes, rotation rates, and modes of motion with precise time intervals, which cannot be captured in high-rate video recording systems and other instrumentation techniques. The sensor data were evaluated with video recordings of the rockfall trajectories at each site. In addition, field measurements of

runout distances were used to evaluate the effectiveness of catchment ditch systems under different slope conditions.

The Smart Rock sensor was also used to instrument small-scale energy restitution experiments. A preliminary laboratory experimental campaign was carried out, dropping a standard block on sand and rock from a constant drop height of 2.2 m. A frontal and upper camera system was implemented to estimate the scalar velocity of the released block in three directions. Bounce heights, scalar velocity estimates, and rotational velocity measurements were used to estimate velocity- and energy-based coefficients of restitution for sand and rock. These experiments have formed the basis of a detailed parametric assessment of rock bouncing parameters.

The field experiments conducted at two of the New Hampshire test sites were compared with two-dimensional simulations. The slope profile for each model was obtained from three-dimensional point clouds of the test slopes, whose cross-sections were extracted based on video observations of the field trajectories. Default coefficients of restitution typically used in 2D simulations were evaluated, as well as the coefficients obtained in the laboratory for sand and rock.

6.2. Conclusions

The following conclusions can be made or confirmed with this research:

Experimental rockfalls with the Smart Rock sensor were successful at the ten proposed test sites:

- The Smart Rock accurately recorded acceleration, rotational velocity, and altitude from the perspective of the falling rock, even in rare cases when the sensor was ejected after rock fragmentation. The video tracking measurements were compatible with the added altitude sensor, whose measurements were useful to identify the time intervals of the rockfall experiments precisely.

The Smart Rock measurements were used to evaluate rockfall modes of motion under different test characteristics:

- Falling block behavior:
    - Acceleration and rotational velocity measurements from a Smart Rock were used to describe the modes of motion of a falling block. The results show that Smart Rock data output patterns could be used to successfully distinguish rockfall motion over time (free fall, bouncing, rolling, sliding).
    - The video measurements validated the SR data and were used to help identify patterns for modes of motion in the Smart Rock data. The colors used at each test rock allowed to visualize changes in rotation direction along the rockfall trajectory.
    - Predominant rockfall modes of motion were identified at different ranges of slope angles. Blocks tended to roll and bounce at grassy slopes between 20º and 30º, bounce on rock slopes between 40º and 60º, describe a transition between bouncing and free falling between 60º and 65º, and predominantly free fall at rock slopes steeper than 65º. These ranges were compatible with field and model observations published in the literature since the 1960s.
- Block displacements:
    - Rock bouncing against the rock face typically increased lateral displacements and runout distances, especially at higher rotation rates. In addition, blocks with higher horizontal velocities towards the road (developed in shallower slope angles) tended to develop further runout distances.
    - Except for one test slope in Franklin (50º inclination), all tests had average lateral dispersions less than 20% of the slope lengths. The measured dispersions agree with

ranges published in the literature. While trends could not be observed for runout distances, the data measurements suggest that lateral dispersion increases at less inclined slope angles. Both runout distances and lateral dispersion can increase after impact on slope irregularities (launch features). Significant bounce heights do not necessarily imply longer runout distances.

  - The most concerning rock cuts were those with shallow slopes (below 50º) and narrow catchment ditches. The experiments have shown that most A-rated cuts were not fully effective to prevent rockfalls from reaching the road, while the B- and C-rated slopes were successful in mitigating rockfall hazard.

- Accelerations and impact forces:
  - Acceleration magnitudes as low as 5 g resulted in significant increases in rotation.
  - The maximum impact force on a rockfall typically occurs upon impact against the rock face or stiffer material at the ground level (asphalt and rock talus). The acceleration measurements can be described using physics principles. Objects dropped onto rigid and less deformable surfaces are expected to achieve higher acceleration levels than softer materials.
  - Rocks of lower mass experienced higher acceleration magnitudes in both field and laboratory experiments. Higher acceleration magnitudes occurred on taller slopes with predominant free fall behavior and less inclined slopes where significant bouncing occurred.
- Block rotation:
  - The Smart Rock data demonstrated how block rotation is sensitive to changes in boundary conditions. Factors as simple as contact with thin tree branches or

accelerations as low as 5 g can significantly increase the rotation rate of a falling block.

- Blocks of smaller mass were more easily subjected to changes in rotation. This behavior could be associated with the difficulty in rotating blocks with higher mass (higher moments of inertia).

The experimental setup in the laboratory was successful in developing a preliminary methodology for energy assessments of falling blocks using a Smart Rock sensor:

- Experiments on sand and rock were successfully conducted to obtain energy- and velocity-based coefficients of restitution for subsequent modeling assessments.
- Impacts on rock have experienced higher acceleration levels compared to sand.
- The results suggest that block dispersion increases as the stiffness of impact surfaces increase. It was observed that a slight inclination at the point of contact on rock influenced the bouncing direction in the three tests performed.
- The alteration in block shape during the tests on sand produced significant differences in energy restitution between the cubic blocks and the cuboctahedron. The cubic block had lower embedment depths compared to the cuboctahedron, thus experiencing higher acceleration levels. Along with deeper embedment, the cuboctahedron experienced a higher lateral dispersion and rotation after impact. While small bounce heights could be measured for the cubic block, the cuboctahedron did not describe visible rebound.
- Higher coefficients of restitution were obtained for the cubic block compared to the cuboctahedron, which displayed nearly zero restitution, implying that the block geometry plays an important role in the restitution upon impact against soft materials. The estimated COR values for both sets of tests agree with previous studies but are significantly lower

than default modeling coefficients. Although past studies in the literature have been published with nearly zero restitution, the author advises against using restitution coefficients approximately equal to zero without previous field assessments, as they can lead to underestimated trajectories.

- Energy restitution on deformable grounds is complex and requires further investigation. Observations from the tests on sand agree with results obtained by Heidenreich (2004), in which the block rebound behavior on granular material is governed by block penetration, sliding, and rotation.
- Based on a limited number of drop tests on rock, the estimated coefficients of restitution were found lower compared to those published in the literature.
- The designed laboratory methodology has a high potential to evaluate bouncing behavior through instrumented tests on different impact surfaces at a range of surface inclinations and drop heights.

The preliminary two-dimensional modeling assessments were successfully compared to the experimental measurements:

- The rockfall simulations performed with both default and laboratory-based coefficients of restitution demonstrated that the modeling software correctly estimates the modes of motion during a rockfall.
- Similar ranges of rotational velocity before ground impact were observed in most models for both sets of coefficients of restitution.
- The laboratory-based coefficients of restitution reproduce more realistic bounce heights compared to the default coefficients. However, the rotational velocities and runout distances after ground impact were overestimated in all simulations.

The research conducted as part of this thesis showed that the measured three-axis acceleration data could be used to calculate resultant acceleration magnitudes. Resultant accelerations were used to estimate impact forces, useful in the design of protective structures, especially at less inclined slopes. In addition, the measured rotational velocity data can be used to calculate the rotational kinetic energy of a falling block accurately with known moments of inertia.

The findings of this study confirm that rockfall events are unpredictable and require further investigation and kinetic energy estimates from the perspective of the falling rock for safer and more economical protective designs. The physical motions described by bouncing and rolling phenomena are the least understood by rockfall studies, given the significant number of variables regarding impact conditions and rock characteristics. Therefore, the increasing demand for more realistic modeling input parameters is associated with public safety as a primary factor and saves time and resources, redirecting to a higher number of medium-to-high hazard rock cuts.

There is an increasing need to estimate coefficients of restitution capable of realistically predicting the dispersion of falling rocks in typical surfaces, and the Smart Rock can be considered a promising tool for accurate energy assessments and consequent hazard mitigation. Observations from this experimental research have demonstrated that similar block sizes can experience significant ranges of motion depending on the slope conditions, primarily controlled by the slope angle and/or presence of launch features. Therefore, the protective design of rockfall events must primarily account for the slope conditions and alternatives to attenuate potential damage upon impact. Catchment ditch widths and geometries, and other safety measures must be engineered to stop falling blocks considering the slope angle and expected type of motion at a specific site.

REFERENCES

Apostolov, A. (2016). Development and testing of motion tracking "Smart Rock" devices for geotechnical applications. (Master's thesis). University of New Hampshire, Durham, NH.

Apostolov, A. and Benoît, J. (2017). Motion Tracking "Smart Rock" Device for the Study of Landslide and Debris Flow Mechanisms. North American Symposium on Landslides. Roanoke, VA, June 4-8.

Asteriou, P., Saroglou, H., and Tsiambaos, G. (2012). Geotechnical and kinematic parameters affecting the coefficients of restitution for rock fall analysis. International Journal of Rock Mechanics and Mining Sciences.

Azzoni, A., and de Freitas, M. H. (1995). Experimentally gained parameters, decisive for rock fall analysis. Rock mechanics and rock engineering, 28(2), 111-124.

Azzoni, A., La Barbera, G., and Zaninetti, A. (1995). Analysis and prediction of rockfalls using a mathematical model. International journal of rock mechanics and mining sciences & Geomechanics (Vol. 32, No. 7, pp. 709-724).

Cassidy, G. (2013). Embedded Pressure and Accelerometer "Smart Rock" for Debris Flow Studies. (Master's thesis). University of New Hampshire, Durham, NH.

Caviezel, A., and Gerber, W. (2018). Brief Communication: Measuring rock decelerations and rotation changes during short-duration ground impacts. Natural Hazards and Earth System Sciences, 18(11), 3145-3151.

Caviezel, A., Christen, M. Buhler, Y. and Bartelt, P (2017). Calibration methods for numerical rockfall models based on experimental data. 6th Interdisciplinary Workshop on Rockfall Protection. May, Barcelona, Spain.

Chau, K. T., Wong, R. H. C., Liu, J., and Lee, C. F. (2003). Rockfall hazard analysis for Hong Kong based on rockfall inventory. Rock Mechanics and Rock Engineering, 36(5), 383-408.

Disenhof, C. R. (2018). Investigation of Surface Models and the Use of a Smart Rock for Rockfall Modeling. (Master's thesis). University of New Hampshire, Durham, NH.

Garcia, B. S. (2019). Analyse des mécanismes d'interaction entre un bloc rocheux et un versant de propagation: application à l'ingénierie (Doctoral dissertation). Université Grenoble Alpes, Grenoble, France.

Gullison, M. (2013). Analysis of Smart Rock data from debris flow experimentation. (Master's thesis). University of New Hampshire, Durham, NH.

Harding, M. (2011). Design and development of a debris flow tracking "Smart Rock". (Master's thesis). University of New Hampshire, Durham, NH.

Harding, M. J., Fussell, B. K., Gullison, M. A., Benoît, J., and de Alba, P. A. (2014). Design and testing of a debris flow 'smart rock'. Geotechnical Testing Journal, 37(5), 769-785.

Heidenreich, B. (2004). Small- and Half- Scale Experimental Studies of Rockfall Impacts on Sandy Slopes. (Doctoral thesis). École Polytechnique Fédérale de Lausanne, Lausanne, Switzerland.

Higgins, J.D., and Andrew, R. D. (2012). "Rockfall types and causes." In Turner, A.K. and Schuster, R.L. (Eds). Rockfall Characterization and Control (pp. 21-55). Washington, D.C.: Transportation Research Board.

Labiouse, V., and Heidenreich, B. (2009). Half-scale experimental study of rockfall impacts on sandy slopes. Natural Hazards and Earth System Sciences, 9(6), 1981-1993.

Leonhardt, P. M. (2001). Acceleration levels of dropped objects. Endevco Corporation.

Peng, B. (2000). Rockfall Trajectory Analysis – Parameter Determination and Application (Master's thesis). University of Canterbury, Christchurch, New Zealand.

Pierson, L.A., Gullixson, C.F., and Chassie, R.G. (2001). Rockfall Catchment Area Design Guide. Report FHWA-OR-RD-02-04m, Oregon Department of Transportation, Dec. 2001.

Ritchie, A.M. (1963). Evaluation of Rockfall and Its Control. Highway Research Board, N. 17, pp 13-28.

Turner, A.K., and Duffy, J.D. (2012). "Evaluation of Rockfall Mechanics." In Turner, A.K. and Schuster, R.L. (Eds). Rockfall Characterization and Control (pp. 285-333). Washington, D.C.: Transportation Research Board.

Turner, A.K., and Jayaprakash, G. P. (2012). "Introduction." In Turner, A.K. and Schuster, R.L. (Eds). Rockfall Characterization and Control (pp. 3-20). Washington, D.C.: Transportation Research Board.

Wyllie, D.C. (2015). Rock Fall Engineering. New York, NY: CRC Press, Taylor & Francis Group.